Evidence of recurrent mass movement in front of the maximum slip area of the 1960 Chile earthquake: Implications for risk assessment and paleoseismology

Cristian Araya-Cornejo[1,2], Matías Carvajal[3], Jasper Moernaut[4], Felipe González[5], Marco Cisternas[3,6]

[1]Instituto de Geografía, Pontificia Universidad Católica de Chile, Chile

[2]Observatorio de Gestión de Riesgo de Desastres, Universidad Bernardo O'Higgins, Chile

[3]Millennium Nucleus The Seismic Cycle Along Subduction Zones, Chile

[4]Institute of Geology, University of Innsbruck, 6020 Innsbruck, Austria

[5]Chair for Computational Analysis of Technical Systems, RWTH Aachen University, Germany

[6]Instituto de Geografía, Pontificia Universidad Católica de Valparaíso, Chile

Corresponding author: Cristian Araya-Cornejo (c.arayacornejo@gmail.com)

Key Points:

- Historic and geomorphic evidence reveals several mass movements triggered by earthquakes on a riverside zone in south Chile.
- Giant earthquakes in 1575 and 1960 triggered mass movements causing river damming, but those of the latter were larger in quantity and size.
- Evidence presented here suggest rethinking near-future hazards and risks in the Valdivia basin.

Abstract

We present evidence that suggests a new risk scenario for the Valdivia basin in south Chile, located in the area of the magnitude 9.5 1960 earthquake. In 1960, three mass movements, triggered by the earthquake shaking, dammed the upper course of the San Pedro River and threatened Valdivia City until it was opened in a controlled manner by its inhabitants. Published historical accounts indicate that the 1575 earthquake, predecessor of the 1960 event, also triggered a mass movement that dammed the upper course of the river. However, here we reinterpret the published account and present new historical records, which we combined with satellite imagery and field surveys to show that the volume of the landslide in 1575 was smaller than the smallest of those of 1960, yet its outburst flood killed thousands of natives located downstream. Additionally, we characterized different mass movement deposits in the upper course of the San Pedro River, including both ancient and those formed in 1960, and we evaluated the mechanisms that could contribute to their generation at present (e.g. land use). Our results suggest that in the present-day conditions a moderately-sized (Mw ~8) earthquake can be sufficient to cause damming the San Pedro River, which challenges the previous assumption that such phenomena are exclusively related to giant 1960-like earthquakes.

1 Introduction

Gravitational mass movements (including landslides) are a significant hazard in most countries (Keefer and Larsen, 2007). Although the triggering of mass movements (MM) depends on different factors (e.g. heavy rains), earthquakes are documented as their main trigger when seismic shaking reaches a Modified Mercalli Intensity (MMI) ≥VI (Keefer, 1984). The recent history of tectonically active zones shows that earthquake-triggered MM have caused tens of thousands of deaths in densely populated areas (Budimir et al., 2014), and are one of the consequences of earthquakes that have caused greatest economic losses (Alexander, 2012). Additionally, earthquake-triggered MM have the potential for triggering cascading hazards (e.g. damming rivers, tsunamis) amplifying its potential effect (Budimir et al., 2014). An example of this are the recent tsunamis following the Mw 7.5 2018 Palu earthquake (Indonesia), which were generated by a combination of submarine/subaerial MM and coseismic seafloor deformation, killing thousands of people (Carvajal et al., 2019).

The preconditioning of slopes towards failure can be influenced by various secondary factors independent of the ground shaking. These include terrain parameters like morphology (e.g. slope angle and curvature), slope materials (e.g. soil cover, lithology and geological structure), hydrology (e.g. water table level and pore water pressure), geomorphology (e.g. presence of ancient MM deposit) and anthropogenic (e.g. land use) conditions (Gorum et al., 2011). Despite their inherent complexity, the empirically-derived causal relationships between earthquake size and mass movements and the preservation of their deposits in the landscape (Keefer, 2013), has allowed to use mass movement deposits as proxies to estimate the ages and magnitude ranges of historical and prehistoric earthquakes (Ojala et al., 2017). Thus, scientific work focused on improving the inventory of earthquake-triggered MM deposits (e.g. spatio-temporal distribution), and/or on characterizing their forcing mechanisms (e.g. terrain parameters), can provide critical information for the assessment of seismic hazard in areas affected by these phenomena (Harp et al. 2011).

Chile is located over one of the most active subduction zones in the world and has one of the higher rates of earthquake occurrence, with an average of two Mw ≥8.4 per century (Ruiz and Madariaga, 2018). Although most of the great earthquakes (Mw >8) are sourced in the megathrust fault formed by the South American and Nazca plates, intraplate faults (e.g. within either plate) have also generated large magnitude events (Mw >6) with associated strong shaking capable of producing MM (Antinao and Gosse, 2009). The Mw 6.2 2007 shallow crustal earthquake in the southern part of the country and its cascading effects provide a remarkable example. Rupturing a ~50 km-long segment of the Liquiñe-Ofqui strike-slip fault (Agurto et al., 2012), this earthquake triggered multiple landslides (e.g. rock slides, rock avalanches, slumps, slow earth flows, others) that entered the Aysén Fjord generating tsunamis that killed a dozen of people (Sepúlveda et al., 2010), highlighting the urgent need of better understanding earthquake-induced MM in Chile and their associated potential hazards. However, aside from a few other MM studies focused on the Mw ~9.5 1960 (Davis and Karzulovic, 1961; Weischet, 1963; Wright and Mella, 1963) and Mw 8.8 2010 (Mardones and Rojas, 2012; Serey et al., 2019) earthquakes, research on this topic in Chile is scarce. The upper course of the San Pedro River (39.7° S, 72.4° W), which originates in the Riñihue Lake, faces the area of maximum slip of the giant (Mw 9.5) 1960 earthquake. This river and lake became the focus of attention after three remarkable MM triggered by the strong 1960 earthquake shaking dammed it. As water accumulated upstream the uppermost dam, the pressure induced to it increased, posing a time-increasing threat to the population living downstream. Fortunately, when the Riñihue Lake level reached about ~26 m above the typical water level, successful interventions leaded by the Chilean government with the collaboration of the inhabitants of the basin (e.g. Valdivia and Los Lagos city inhabitants), prevented an imminent collapse saving tens of thousands of people (Davis and Karzulovic, 1961). A similar story had occurred almost four centuries before, although with more tragic consequences. The historic earthquake of 1575 identified as the predecessor of the 1960 earthquake (Cisternas et al., 2005), also triggered MM that dammed the San Pedro River. However, aborigines living downstream by the time did not face the same destiny. After *"months"* of water accumulation and over ~50 m of water level increase, the dam collapsed and killed *"hundreds"* of them (Montessus de Ballore, 1912). Today, the MM deposits triggered by both earthquakes are identifiable on the land surface and/or along the riverside, and their process and geomorphology has not been investigated in detail. These deposits are the main focus of this paper.

Here we improve the knowledge of earthquake-triggered MM in Chile by an in-depth study of the MM deposits triggered by the 1960 and 1575 giant earthquakes in the upper course of the San Pedro River. Through field observations and satellite imagery combined with newly found historical accounts, we identify the deposits of both events and compare them with previous reports. We further construct a high-resolution terrain model to study their characteristics at different spatio-temporal scales. Finally, we review the potential factors controlling their triggering and discuss the implications of modern land use on the geological hazards in the area.

2 Study Area

2.1 Geographical and seismotectonic setting

The San Pedro River and Riñihue Lake are located in the foothills of the Andes, about 280 km south from the northern end of the 1960 rupture area (Figure 1). It originates in the outflow of

Riñihue Lake and flows into the Pacific Ocean (named Valdivia River). The upper course of the river exhibits geographic and geological characteristics that pose potential hazards for the population living downstream (~160.000 people). Its hydrographic catchment is composed of seven other lakes, five in Chilean territory and two in Argentina, covering an area of ~450 km^2 (Figure 2a). The interconnected system of lakes has a pluvio-nival regime and the river is naturally regulated by these, which generates that a large part of the sediment load transported from the upper catchment is deposited on the bottom of the lakes. For this reason, the San Pedro River has crystal clear waters (Habit and Parra, 2012). Given the extensive hydraulic catchment and their precipitation regime (~2200 mm/yr), landslide damming of San Pedro River could lead to a rapid accumulation of a vast amount of water, potentially leading to catastrophic outburst floods.

The seismotectonic setting is located in the south-central part of the active subduction zone of Chile, which extends for ~3200 km from the northern limit of the country (18.4° S) to the Taitao Peninsula (46.5° S). Along this zone, the Nazca oceanic plate subducts under the continental plate of South America at a relative convergence of ~65-70 mm/year (Angermann et al., 1999). The frictional interaction between both plates induces internal stress and consequent elastic deformation in the upper plate, which slowly accumulates through decades or centuries until it is suddenly released by large megathrust earthquake ruptures (Scholz, 2002).

In the ~500 years of Chile's history, the southern segment of this subduction zone has generated at least five major megathrust earthquakes, including the Mw 9.5 1960 event, the largest instrumentally-recorded worldwide (Kanamori and Cipar, 1974). Other significant earthquakes occurred in 1575, 1737, 1837 (Lomnitz, 1970; Cisternas et al., 2005) and recently in 2016 (Mw 7.6) (Figure 1a,b). Despite the relative temporal regularity between one event and the other, independent analysis of historical documents (Cisternas et al., 2017a) and sedimentary records at the coast (Cisternas et al., 2017b) and within inland lakes (Moernaut et al., 2014), indicate that the 1960 earthquake was only rivaled by the 1575 earthquake in terms of magnitude and rupture extent. In contrast, the smaller 1737 (M ~7.5-8) and 1837 (M ~8.5-9) earthquakes were limited to the northern and southern two thirds of the 1960 rupture area (1000 km long), respectively (Figure 1b) (Cisternas et al., 2017a). The recent well-instrumented 2016 earthquake, with a Mw 7.6 (Moreno et al., 2018), seems to be the smallest event of this historical sequence, rupturing a small, deep patch on the megathrust between latitudes 43-43.5º S (Moreno et al., 2018). Besides these large events, the seismic catalogue shows 26 poorly-constrained events since 1570 with magnitudes apparently over M 7 (white circles in Figure 1a,b), which yield an average of 6.5 events per century in this area.

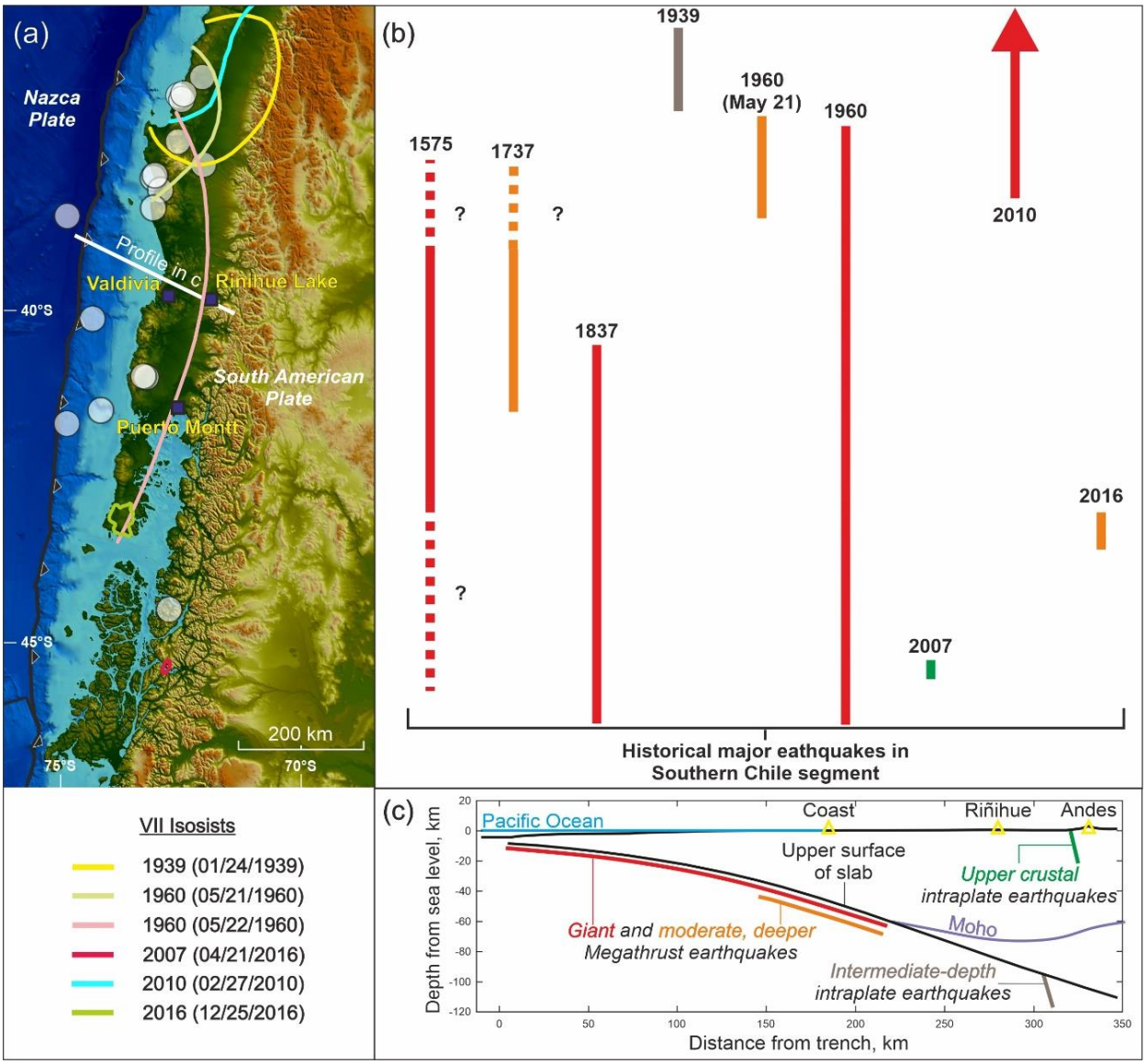

Figure 1. (a) Location of earthquakes larger than Magnitude 7 that striked South-Central Chile in the historical period 1570-2016 (National Seismological Center of Chile, 2019); and Isoseist VII of the intraplate earthquakes of 1939 (Astroza et al., 2002) and 2007 (Vanneste et al., 2018); and interplate earthquakes of 1960 (21 and 22 of May) (Astroza and Lazo, 2010), 2010 (Astroza et al., 2012), and 2016 (USGS, 2016). (b) Rupture lengths of the most significant well-investigated earthquakes along the region. The line colors represent the source type of the earthquakes shown in (c). Orange are moderate-size, deeper interplate earthquakes (1737 (Cisternas et al., 2017a), May 21 1960 (Ruiz and Madariaga, 2018) and 2016 (Moreno et al., 2018)). Red are great earthquakes rupturing the entire seismogenic width (1575, 1960 (Cisternas et al., 2005) and 2010 (Moreno et al., 2012)). Green indicates the strike-slip rupture of the 2007 earthquake along the Liquiñe Ofqui Fault Zone (Agurto et al., 2012). Light brown indicates the 1939 intermediate-depth earthquake rupture within the subducted slab (Beck et al., 1998).

Although no strong shaking has been instrumentally recorded in the direct vicinity of the San Pedro River, its relatively close location to the different earthquake source types in Chile makes

it an exposed site for seismic shaking. Because it is located ~280 km from the trench and over the local downdip limit of the megathrust seismogenic zone, it is exposed to great-to-giant megathrust earthquakes (Mw >8.5), rupturing the entire seismogenic zone width (e.g. 1960 and 2010 type earthquakes), but also to smaller ones (Mw ~8) if are generated by deep interplate ruptures (e.g. Mw 7.6 2016 earthquake). Although smaller in magnitude, earthquakes rupturing near the bottom of the seismogenic zone are capable of producing strong, high frequency shaking radiated from these interplate depths (Lay et al., 2012). The Mw 7.6 2016 Melinka earthquake, for example, caused MMI VII over its rupture area (USGS, 2019). According to Moreno et al. (2018), earthquakes with these characteristics will continue to occur along this region while strain energy builds-up for the next 1960-type earthquake. Additionally, because the San Pedro River is only a few tens of kilometers from the trace of the Liquiñe-Ofqui strike-strike slip fault zone, it can also be exposed to strong shaking from these events. The Mw 6.2 2007 Aysén earthquake, with the associated landslides and tsunami effects, represents a recent example of this type of earthquakes. Strike-slip faults are well-known to cause very strong shaking (>VIII MMI) near and around the rupture area, even in moderate-size earthquakes (Carver et al., 2004; Colombelli et al., 2013; Symithe and Calais, 2016; Barnhart et al., 2019).

Finally, the San Pedro River is also exposed to potential shallow earthquakes originating at the Andes foothill (e.g. Alvarado et al., 2009) and to intermediate depth events generated within the downgoing slab (Beck et al., 1998) (Figure 1c). The latter type of events are capable to produce very strong shaking with epicentral seismic intensity of up to MMI IX (Moya, 2002). In fact, the largest seismic catastrophe in Chile, with about ~20.000 deaths, was caused by the Ms~7.8 Chillán intermediate-depth earthquake (Beck et al., 1998; Ruiz and Madariaga, 2018).

2.2 Geological setting and previous work

The local geological setting of the upper course of the San Pedro River is a relevant factor to explain the presence of MM deposits triggered by earthquakes. The riverside zones of its middle and upper courses show multiple MM deposits, which cover an approximate area of 10 km^2 (Figure 2b). They are identifiable with any remote sensing tool due to their size and exhibit a well demarcated outline. Some of these deposits are coalescent and show different degrees of evolution, evidenced by their level of surface roughness and the escarpments slope gradients. Also, these deposits can determine the sinuosity of the river. Due to their morphological features, such as roughness and size, the MM deposits of the middle course of the San Pedro River are clearly older and smaller than those present in the upper course (Figure 2b). Interestingly, these phenomena have not been recorded either geomorphologically or historically in neighboring basins of tributary rivers, despite their similar seismic exposure and climatic conditions (e.g. Quinchilca and Bueno rivers, Figure 2b).

The local stratigraphy at the upper river course is formed by deposits originating in glacio-lacustrine and glacio-fluvial environments, inherited from the last glacial and interglacial periods, and the current postglacial. Rodríguez et al. (1999) indicate that in this zone the moraine deposits intercalate with glacio-fluvial sediments and glacio-deformed laminated silts, which was also observed by Davis and Karzulovic (1961) in the scarp that generated the largest slide of 1960 (~60 m, Figure S1a). Results of laboratory tests performed on sediments obtained from two drillings, showed that some of the strata are susceptible to liquefaction (Noguera and Garcés, 1991). These authors propose that the deposits that were liquefied during the 1960 earthquake

correspond to perturbed silty strata with some sands and gravels, observable at ~28 m depth. This type of sediment combination (silt, sand and gravels) can also be seen in the scarp, between ~19 and 29 m deep (Figure S1b).

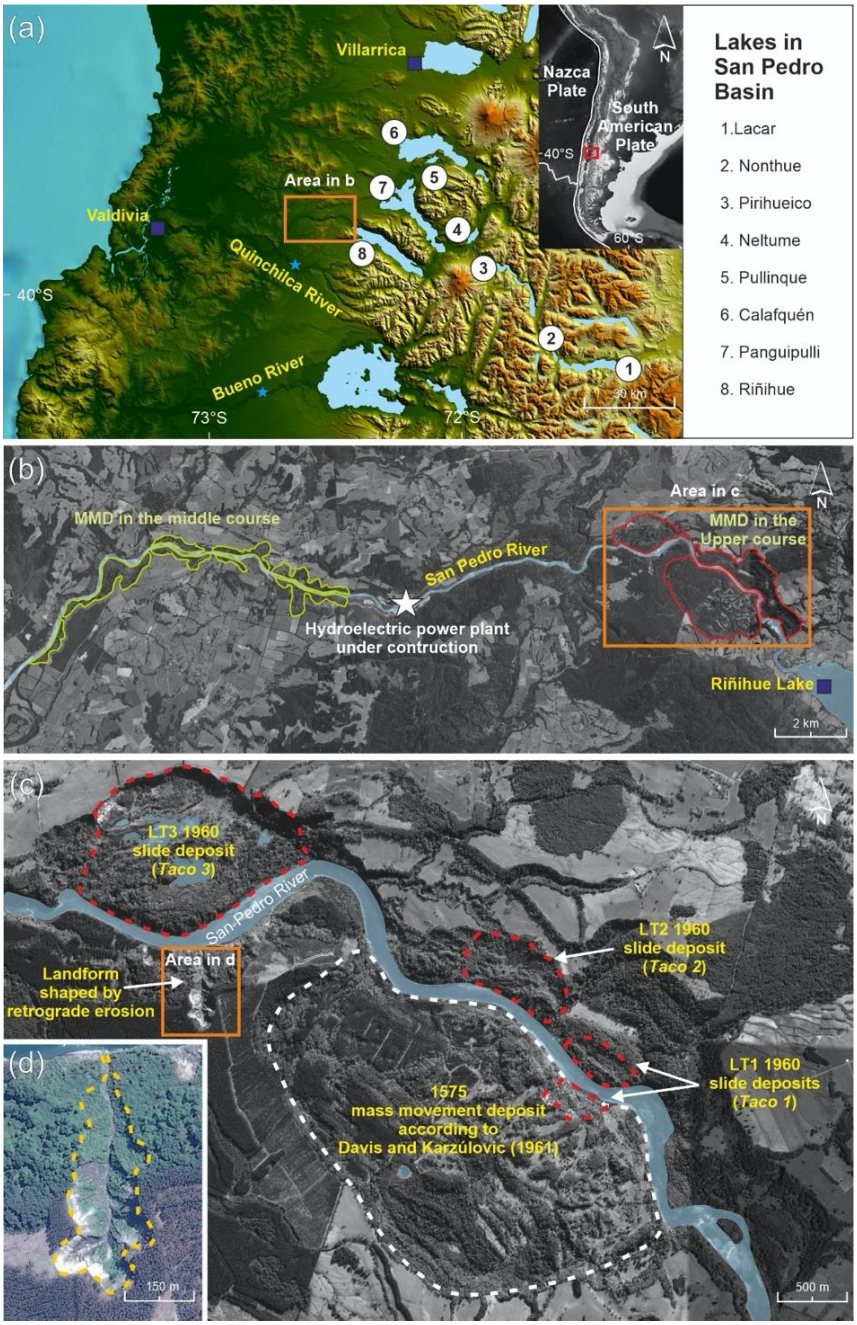

Figure 2. (a) Study area and San Pedro basin. (b and c) MMDs in the upper and middle course of San Pedro River. (d) Landform shaped by retrograde erosion generated by improper management of land use after the 1960 earthquake.

3 Materials and Methods

3.1 Historic archives

We conducted a research of historical sources to improve our knowledge about the MM deposits that dammed the San Pedro River in 1575. In addition to reviewing bibliography in recent scientific and historical works, we searched for documents in *the Archivo General de Indias* located in Seville, Spain; the *Archivo de la Nación* located in Lima, Peru; and the *Archivo Nacional* that is located in Santiago, Chile.

The *Archivo General de Indias* has a thousand of documents from Hispanic America, written in the times of the Conquest and Cologne. Most of these documents were addressed to the Kings and the authorities that ruled America from Spain. The *Archivo de la Nación* contains lodged manuscripts generated in the Governorships and Captaincies belonging to the Viceroyalty of Peru, including Chile, and which were directed towards authorities who lived in America as the Viceroy. Finally, the *Archivo Nacional* is the most important historical archive in Chile, and contains records issued to local authorities. In the latter we found three unpublished manuscripts that refer to the MM that dammed the San Pedro River in 1575, and that we describe in Table 1 and in the supplementary material (Texts S1, S2 and S3).

3.2 Spatio-temporal characterization of MM deposits

The MM deposits in the San Pedro River were characterized by combining field observations, satellite images and early geomorphological descriptions of Davis and Karzulovic (1961).

Two fields surveys, conducted in January 2014 and 2015, were focused on the geomorphology and sedimentology characterization of the main MM deposits present in the upper course of the San Pedro River, and also in the outflow of Riñihue Lake. For the analysis of satellite images, we used the Google Earth software and images obtained by the Chilean Air Force in 1961, i.e. a few months after the 1960 earthquake occurred. For the geological description, the study by Davis and Karzulovic (1961) was used, complemented with the geological maps generated by Rodríguez et al. (1999).

We studied the evolution of the larger slide deposit generated by the 1960 earthquake using two topographic profiles obtained by Davis and Karzulovic (1961). Its location was georeferenced by means of a GIS (open source software QGIS) and was compared with two profiles obtained from a cloud of LIDAR points in 2010 (Figure 3a). The LIDAR information was processed with GIS, allowing the removal of the dense vegetation from the surface. As a result of this processing, a Digital Terrain Model (DTM) of 1 m of resolution was generated. The profiles were also obtained from other MM deposits present on the riverside zone of the San Pedro River, using the methodology described above.

3.3 Erosion rate of LT3 scarp

We studied the erosion rate along the largest slide deposit generated by the 1960 earthquake, hereafter referred to as LT3. The Erosion Rate (E), defined as the annual amount of eroded material from the scarp that forms part of LT3, was estimated from:

$$E = \frac{M}{t}$$

(1)

where M is the amount of mass removed from the scarp and t is the elapsed time. The period considered is 50 years, between 1960 and 2010. The input for this calculation was obtained from the two topographic profiles (A-A' and B-B', Figure 4b) reported in the paper of Davis and Karzulovic (1961), and from LIDAR information processed in the GIS. Only the surface of the escarpment was considered. As a result, two values of E were obtained, one for each topographic profile and associated scarp.

Our calculations also considered depth-dependent changes of the density of the deposits that formed the scarp. We use the densities present in Noguera and Garcés (1991), that were obtained by drillings executed on the terrace where LT3 originated, close to main scarp. The density of sediments changes significantly at 16 m depth. Therefore, a density ρ=1.78 tons/m^3 and a ρ=2.38 tons/m^3 was considered for the upper part and for the rest of the scarp, respectively. Finally, the mass removed from the scarp was obtained by computing the weighted average between the eroded volume and its respective density.

4 History of MM that dammed the San Pedro River

4.1 The MM triggered by the 1575 and 1960 earthquakes

The San Pedro River has been dammed at least twice since the beginning of written history of Chile (i.e., 1541). In both occasions the trigger was strong shaking caused by earthquakes; first in 1575 and then in 1960. Although multiple MM were reported for the 1960 earthquake at different locations in south-central Chile (Weischet, 1963; Wright and Mella, 1963), those in the San Pedro River reached public notoriety due to the threat that represented for the population of ~60,000 inhabitants located downstream. Three slides dammed the river. The volumes of sediments removed by these slides were $30x10^6$, $6x10^6$ and $2x10^6$ m^3 (Davis and Karzulovic, 1961). The deposits that dammed the river were called locally as *Taco 3* (LT3), *Taco 2* (hereinafter LT2), and *Taco 1* (hereinafter LT1) respectively (Figure 2c). Through the intervention of the State of Chile (National Electric Company) and the heroic effort of hundreds of locals, the dams were opened in a controlled manner. All these events, and due to the proximity to Riñihue Lake, led to locals call this historic event as *Riñihuazo*.

In 1575, however, the population was severely affected, mainly those that lived on the riverside zone. The historical chronicles compiled by Montessus de Ballore (1912) and Cisternas et al. (2005) describe that the formation of the natural dam caused water accumulation for nearly five months, collapsing catastrophically and the resulting outburst flood taking the lives of *800* to *1200* aborigines, according to data estimated by colonial authorities and witnesses. However, none of the authors of the chronicles compiled by Montessus de Ballore described the MM that blocked the river. Based on morphological features, Davis and Karzulovic (1961) proposed that one of the deposits present in the upper course of the San Pedro River, which triples in size to LT3, corresponds to the MM occurred in 1575 (Figure 2c). However, the historical evidence presented below does not match with what was proposed by these authors.

4.2 Historical evidence of the characteristics of the MM of 1575

Our bibliographic and archive search resulted in nine historical documents that refer to the deposit of 1575 event (Table 1). Among these, one written by an anonymous author provides the

281 only direct observations of the MM deposit when the San Pedro River was still dammed. The
282 report describes both its size and location. Interestingly, both the size and location inferred from
283 this first-hand account do not coincide with those suggested by Davis and Karzulovic (1961)
284 based on morphological appearances. The MM deposit suggested by these authors is located 2
285 km away from the outflow of Riñihue Lake (Figure 2c). However, the eyewitness reported a
286 location right in the outflow of Riñihue Lake, and an associated volume of ~$1.2x10^6$ m^3 and an
287 area of ~1,5 ha (according to the official measurement unit used in those years (e.g., De Ramon
288 and Larraín, 1979)), which is about half the volume of LT1 and ~200 times smaller than the
289 landslide proposed by Davis and Karzulovic (1961). Seven other secondary sources support the
290 location reported by the eyewitness (Table 1).

291 Table 1

292 *Historical data obtained from settlers of the MM of 1575*

Type of historical source	Author	Place of origin	Date	Eyewitness?	N° of MM described	Location	Size of MM	Lake level rise	Source
Letter	Pedro Feyjó	Valdivia	12/28/1575	No	1	Outflow of Riñihue Lake	-	-	in Cisternas et al., 2005
Letter	Cabildo de la Imperial	La Imperial	01/08/1576	No	2	Outflow of Riñihue Lake	-	-	in Cisternas et al., 2005
Letter	Martín Ruiz de Gamboa	Concepción	02/12/1576	No	-	Outflow of Riñihue Lake	-	-	in Cisternas et al., 2005
Letter	Francisco de Gálvez	Santiago	02/21/1576	No	2	-	-	-	Unpublished. See in supplementary Text S1
Relation	Anonymous	-	Between dec. 1575 and apr. 1576	No	-	Outflow of Riñihue Lake	-	~70 m	in Silgado, 1985
Letter	Antonio Carreño	Santiago	08/10/1576	No	-	Outflow of Riñihue Lake	-	~80 m	Unpublished. See in supplementary Text S2
Relation	Antonio Carreño	Santiago	10/10/1576	No	-	Outflow of Riñihue Lake	-	~80 m	Unpublished. See in supplementary Text S3
Chronicle	Pedro Mariño de Lobera	Santiago	-	No	1	Outflow of Riñihue Lake	-	-	in Montessus de Ballore, 1912; in Cisternas et al., 2005
Relation	Anonymous	Arauco Province	Between 1576-1598	Yes	1	Outflow of Riñihue Lake	~$1x10^6$ m^3*	~50 m	in Silgado, 1985

*1x1 quarter pace and 30 "*estados"* high.

5 Characteristics and evolution of LT3

5.1 The sliding process

The deposit of LT3 was generated by a multirotational slide (Hauser, 2002). At the time of its formation the slide generated an average scarp of 40 m. The slide deposit was made up of a debris apron, a series of failed and rotated blocks, a large unitary block, folds, and a terminal zone or toe, corresponding to the propagation front that went towards the San Pedro River (Figure 3a). The toe and the unitary block were the sections of slide that dammed the riverbed. The toe was eroded by the river after the works carried out for the controlled opening of the *Tacos*, modifying the original course.

In the first months after the slide, important erosive processes and deposits such as pediments, cones, fans, deltas, drainage systems and block rounding were observed (Davis and Karzulovic, 1961). This was caused by the abundant precipitation, the initial absence of vegetation and the presence of a large number of water springs that arose from the different porous sediments of the escarpment wall, discharging water towards the slide deposit.

5.2 The Evolution of LT3

The profiles presented in Figure 3c show that, in 50 years, the landform show important changes is the main scarp, since it shows a notable setback and a decrease in its slope gradient (see section 5.3). The other main structures of the landslide deposit, such as the rotated blocks and the unit block, have been preserved without major changes. Only a softening and lowering of its slopes is observed. Some lagoons formed in 1960 still persist, while the others have been filled with sediments and/or drained. Moreover, vegetation coverage has increased in height and density. The bed of the San Pedro River is displaced towards the south for about 70 m (Figure 3c), possibly caused by a lateral displacement of the slide deposit. This phenomenon, in conjunction with the occurrence of dams, indicates that the upper course of the San Pedro River undergoes significant modifications in its shape and axis due to earthquake-triggered MM and the post-depositional mobility of the MM deposits.

5.3 Scarp retreat

The scarp of the B-B' profile has a higher erosive rate than the scarp of A-A' (Figure 3c). The A-A' scarp presents an average erosion rate of 39 tons/year per linear meter of scarp, while the B-B' scarp averages a rate of 58 tons/year. This erosive rate is also reflected in the slope changes experienced by the escarpment: from 71° to 43° for A-A', and from 75° to 37° for B-B'. It should be considered that the escarpment of the B-B' profile had a greater height (10 m) and slightly steeper initial gradient.

According to descriptions of Davis and Karzulovic (1961), it is inferred that in 1960 the erosion index was much higher than the averages described above, because at present the same erosive phenomena described by these authors are not observed (see section 4.1). The difference and variability between erosive indices hampers the morphologic dating of the MM deposits in the study area, due to more homogeneous value is needed in a scarp formed at the same time or

event. Additionally, some escarpments can be reactivated and/or accelerate their erosive processes with the occurrence of earthquakes subsequent to their formation (see section 6.1).

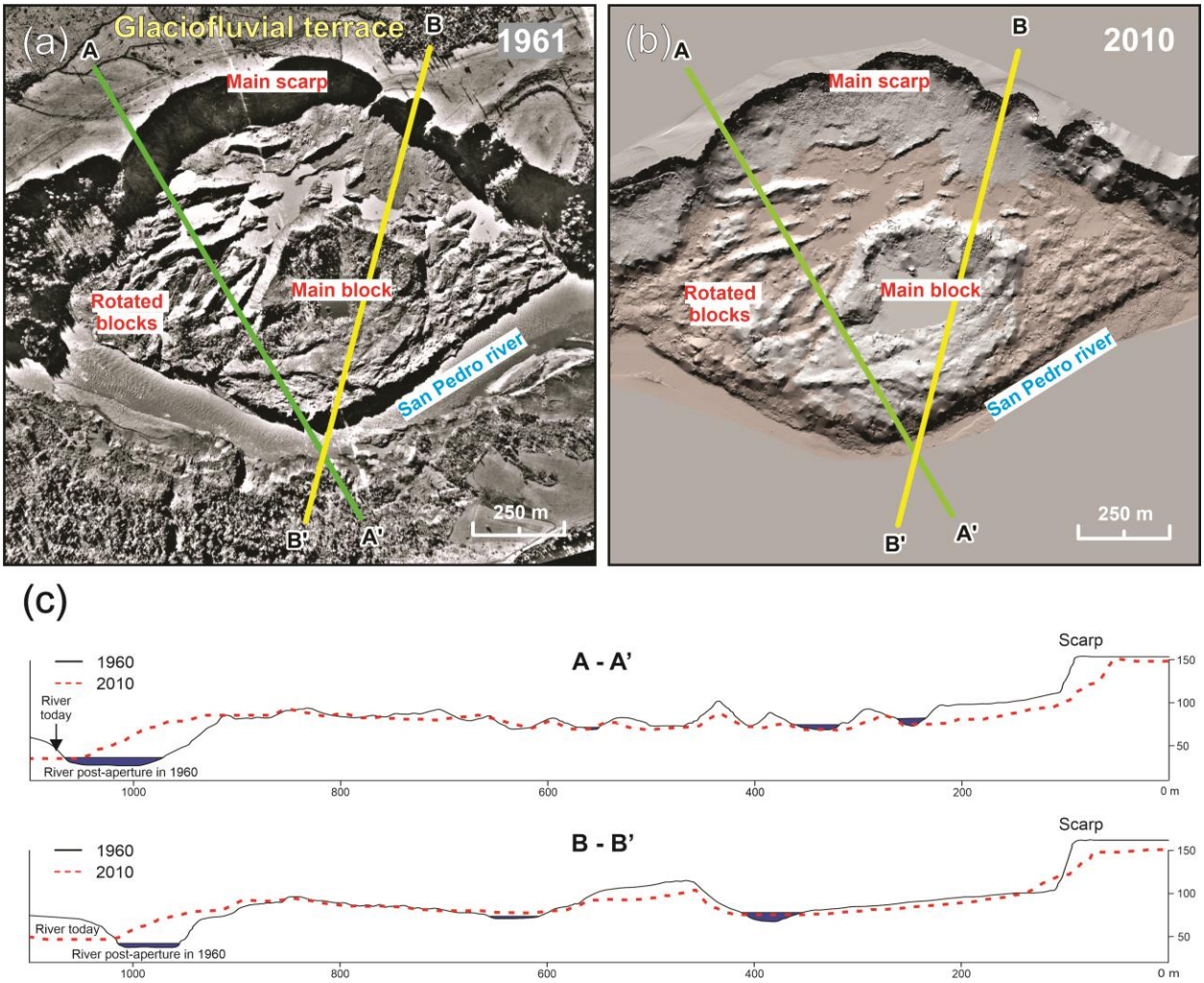

Figure 3. (a) LT3 main geomorphological features in aerial photography (Chilean Air Force, 1961) and (b) 2010 LT3 DTM LIDAR-based information. (c) Topographic profiles (profiles lines in A and B) obtained from Davis and Karzulovic (1961) (A-A'/B-B') compared to profiles obtained from LIDAR-based information.

6 Ancient MM deposits as evidence of recurrent earthquakes

6.1 Characteristics of ancient MM deposits in the San Pedro river upper course

By screening historical documents, we could not find evidence of other processes of dam formation (and subsequent outburst floods) in the San Pedro River other than by earthquakes. This leads us to believe that the ancient deposits (generated before 1960) in the riverside zone of the San Pedro River were also formed by earthquakes. Morphological similarities with those generated in 1960 further support this suggestion.

Traces of the ancient deposits, potentially associated to earthquake-induced MM, are shown in Figure 4. Among their main characteristics, they feature escarpments of 20 m or more with slopes above 30° and exhibit a slide body that projects into the river with one or more ridges. Two of the ancient MM deposits (visualized in B-B' and C-C' profiles, Figure 4b) were modified by the 1960 earthquake, because the slides that generated the LT1 were formed on a section of these (Figure 4c). In contrast, the deposit of the LT2 represented in the D-D' profile (Figure 4b) was originated entirely by the 1960 earthquake. The deposits represented by the A-A' and E-E' profiles in the Figure 4b have morphological characteristics similar to the other deposits previously described, and presented reactivations of their scarps during the 1960 earthquake, which can be observed for the E-E' profile in Figure 4b. All the elements described above suggest that, although some deposits may have been formed in a single event, others were caused by remobilizing preexisting MM deposits.

This data suggests that a MM deposit can be formed by one or more events generated at different times. If the historical antecedents (size and location) are considered, the proposal of Davis and Karzulovic (1961) for the 1575 MM becomes even more debatable, because the proposed deposit can be made up of more than two events. The deposit represented by A-A' profile in Figure 4b is located closer to the Riñihue Lake outflow and its section bordering the river could be considered as a more possible candidate for the 1575 river-damming MM deposit. This hypothesis considers the morphology, the size and the location revealed by the historical evidence, in addition to the presence of an island as a typical characteristic of MM deposits in this locality (section 6.2; Figure 5).

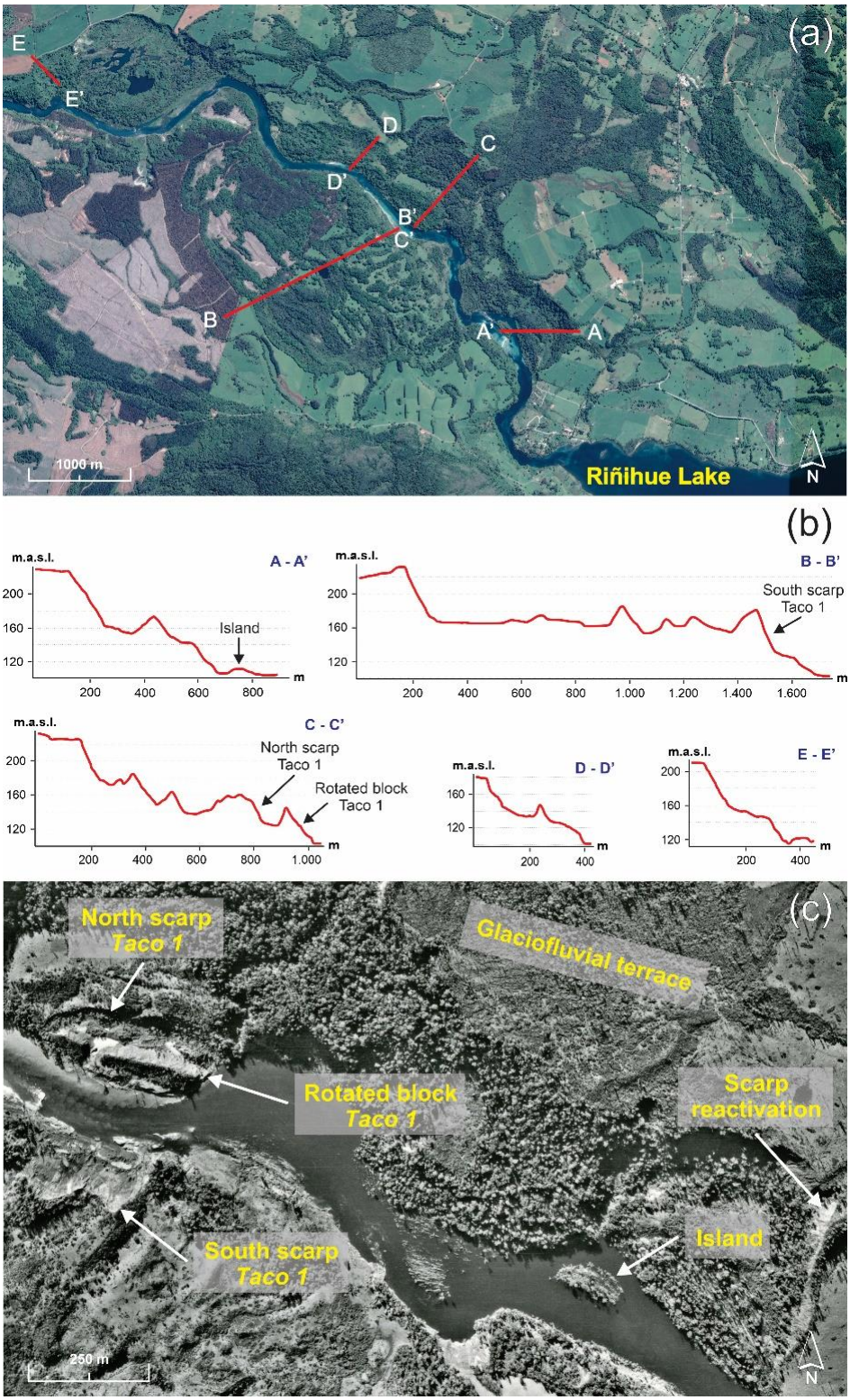

Figure 4. (a and b) MM deposit profiles in San Pedro River upper course. (c) Scarps of slide deposit that generated LT1 and evidence of reactivation of scarps of ancient MM by the 1960 earthquake (Aerial photography from Chilean Air Force, 1961).

6.2 Islands as evidence of ancient MM?

The islands along the upper and middle course of the San Pedro River may have been formed from ancient MM as well. Similar islands formed by MM have also been observed by Hewitt (1998) in the upper course of the Indus River in Pakistan. One of the islands in the upper course of the San Pedro River was investigated in the field and has characteristics that suggest a colluvial and non-fluvial origin. Its location (facing an ancient MM deposit), size, geological composition, and the low sediment load of the river support this proposal (island in Figure 5b and 5c).

The island currently has an area of ~1.4 ha, a height of ~4 m above the average water level of the river and shows a dense vegetation on its surface. The island existed before the 1960 event (Figure 4c), so it resisted at least partially, the increase in the water level and controlled discharge in the river during the *Riñihuazo*. Its presence is remarkable considering that the upper course of the San Pedro River is devoid of sediment load as Riñihue Lake and the other lakes upstream act as sediment traps. This situation, combined with other factors such as slope and average flow (1% / ~400 m^3/s) determine the presence of bedforms, such as middle and lateral banks. The island deposits consist of glaciofluvial terrace material and morainic deposits, which is similar to MM deposits located alongside the San Pedro River. This idea is supported by the granulometric variability (very poor sorting) and the existence of rounded to sub-rounded blocks in a matrix of fine sediments (silts and clays) and gravels (Figure 5b and 5c).

All in all, these observations may suggest that this island was part of an ancient MM that could have dammed the San Pedro River. Also, it leads us to suggest that the other islands located further downstream, which face ancient MM deposits, are vestiges of these and not fluvial deposits.

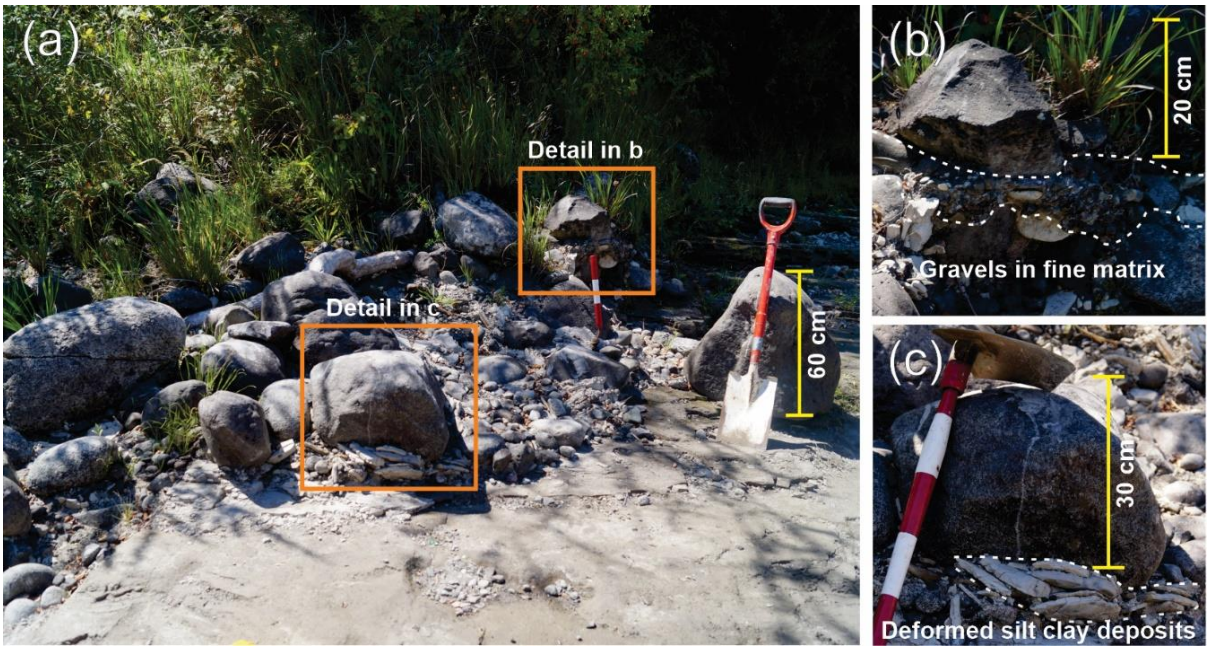

Figure 5. Deposits in an island in the upper course of San Pedro River suggesting that is was formed by an ancient MM that dammed the river.

7 Factors that affect the generation of MM in the San Pedro River

As reviewed in the previous sections, the 1575 and 1960 earthquakes must have generated sufficient local intensities to trigger MM capable of damming the upper course of San Pedro River. Stronger shaking from these events, compared with the rest of the historical sequence, is consistent with the turbidite record in Riñihue Lake and other nearby lakes (Moernaut et al., 2014). Based on the similar thickness and distribution of the 1575 and 1960 turbidite deposits, Moernaut et al. (2014) inferred seismic intensities of about MMI VII½ for the 1575 earthquake in Riñihue Lake. On the other hand, in the 1737 and 1837 earthquakes there were no MM that dammed the San Pedro River, and coincidentally, the inferred seismic intensities based on the Riñihue Lake sedimentary record were smaller (about VI½) for these earthquakes (Moernaut et al., 2014).

Considering these facts, from the point of view of the analysis of Natural Hazards it is necessary to ask: What are the factors that influence the triggering of MM in the upper section of the San Pedro River, and what are the scenarios capable of triggering MM in this zone? If we assume that geological and seismic conditions are relatively constant in a period of a few millennia, then it is reasonable to consider climate seasonality, transient climatological events (e.g. ENSO events), geomorphological evolution and land use as factors that affect the generation, quantity and dimensions of MM. In the case of the San Pedro River, the incidence of the seasons and land use can be evaluated, because although Moernaut et al. (2014) assign similar seismic intensities between the earthquakes of 1575 and 1960, the historical evidence reveals variations regarding the quantity and size of the MM that they generated. If we consider the testimony of the only known eyewitness (see 4.2 section), the 1575 earthquake generated a single MM deposit that reached an approximate dimension of about 1.2×10^6 m^3, equivalent to half the size of the slide generated by LT1, and 1/30 of LT3.

The area in which the upper course of the San Pedro River is located is one of the rainiest in south-central Chile. According to the Chilean General Direction for Water, it rains annually ~2200 mm, focused mainly during autumn and winter (Riñihue Lake station, General Direction for Water, 2019). The 1960 earthquake occurred in autumn on May 22, and the annual rainfall accumulated up to that date was 580 mm (Chilean Meteorological Direction, 2019). This amount of accumulated rainfall favored a saturation of the fine sensitive strata, being decisive for the generation of slides on nearly-horizontal strata (Noguera and Garcés, 1991). In contrast, the event of 1575 occurred in December 16, that is, entering the summer, so that strata may have been saturated to a much smaller degree than in case of the 1960 event. Possibly, these seasonal variations partly explain the differences in quantity and size of deposits generated by the events of 1575 and 1960.

As was recently demonstrated by the September 2018 Mw 7.5 earthquake in Sulawesi, Indonesia, inefficient land use management combined with strong shaking events can cause catastrophic consequences for the population due to MM (Watkinson and Hall, 2019; Bradley et al., 2019). In general, less vegetation cover on non-rocky slopes condition the saturation of the strata and the water table, making them more susceptible to failure (Wu and Sidle, 1995). In 1575, there is no evidence of settlements or significant extractive activities in the upper course of the San Pedro River, neither Spanish nor indigenous, so the forest vegetation was practically pristine (Solari et al., 2011). Whereas for 1960, the aerial photographs show grasslands with

subdivisions and soil with scarce arboreal vegetation (agricultural use), as can be seen in the glaciofluvial terrace where LT3 was formed (Figure 3a). Therefore, it is reasonable to think that the slopes and surfaces in 1575 could have been less susceptible to failure than in 1960, as a result of the greater vegetational coverage and the better condition of the soils, which in turn allowed for less infiltration and saturation of pores in the strata. These differences suggest that the MMs that originated the *Riñihuazo* in 1960 may not have occurred in such quantity and magnitude if the earthquake would have occurred in a drier season and/or with less human intervention, as in 1575. In any case, MM and river damming occurred regardless of the season or land use, so these aspects may be less important than the seismic or geological factors.

8 Conclusions

Here we suggest that in the present conditions not only a giant earthquake (Mw 9-type) like in 1575 or 1960 is needed to dam the San Pedro River, but that also a medium-size earthquake (Mw about 8) could do this. We base this on the following reasoning: i) the geological conditions of the upper course of the San Pedro River which facilitate the development of slope failures and reactivations of MM deposits; ii) the current seismic condition of the Valdivia segment that has already the potential to generate earthquakes of magnitude ~8 (Moernaut et al., 2018; Moreno et al., 2018); iii) the precipitation regime (~2200 mm/yr) with excessive rainfall in winter; iv) the land use which has caused the development of a significant landform (4 ha) shaped by retrograde erosion, generated by improper management (Figure 2c and 2d); v) and the historical evidence that shows us that relatively small MM can dam the San Pedro River, such as the LT1 of 1960 and the MM deposit described in 1575.

The evidence presented here has important implications for the engineering design and emergency plan (in case of a new landslide dam and potential outburst flood) of the hydroelectric power plant located 6 km downstream of LT3, and that is currently being evaluated by the Chilean Environmental Assessment System.

9. Acknowledgments

C.A.C. acknowledges the support of the Doctoral program of Institute of Geography of the Pontificia Universidad Católica de Chile. M.C. acknowledges the support of the Iniciativa Científica Milenio (ICM) through Grant Number NC160025, FONDECYT Project Number 1190258, and the doctoral program of Geological Sciences of the Universidad de Concepción. Special thanks to F. Torrejón for his collaboration in the search for unpublished historical information and his references to information already published.

10. Bibliography

Agurto, H., Rietbrock, A., Barrientos, S., Bataille, K., & Legrand, D. (2012). Seismo-tectonic structure of the Aysén Region, Southern Chile, inferred from the 2007 Mw = 6.2 Aysén earthquake sequence. *Geophysical Journal International, 190*(1), 116-130. doi: 10.1111/j.1365-246X.2012.05507.x

Alexander, D. (2012). Vulnerability to Landslides. In T. Glade, M. Anderson & M. J. Crozier (Eds.), *Landslide Hazard and Risk* (pp. 175-198): John Wiley & Sons, Ltd.

Alvarado, P., Barrientos, S., Saez, M., Astroza, M., & Beck, S. (2009), Source study and tectonic implications of the historic 1958 Las Melosas crustal earthquake, Chile, compared to earthquake damage. *Phys. Earth Planet. Inter., 175*, 26-36. doi:10.1016/j.pepi.2008.03.015

Angermann, D., Klotz, J., & Reigber, C. (1999). Space-geodetic estimation of the Nazca-South America Euler vector. *Earth and Planetary Science Letters, 171*(3), 329-334.

Antinao, J. L., & Gosse, J. (2009). Large rockslides in the Southern Central Andes of Chile (32–34.5°S): Tectonic control and significance for Quaternary landscape evolution. *Geomorphology, 104*(3), 117-133. doi: 10.1016/j.geomorph.2008.08.008

Astroza, M., Moya, R., & Sanhueza, S. (2002). Estudio comparativo de los efectos de los terremotos de Chillan de 1939 y de talca de 1928. Paper presented at the VIII Jornadas Chilenas de Sismología e Ingeniería Antisísmica, Valparaíso, Chile.

Astroza, M., & Lazo, R. (2010). Estudio de los daños de los terremotos del 21 y 22 de Mayo de 1960. Paper presented at the X Jornadas de Sismología e Ingeniería Antisismica, Santiago, Chile.

Astroza, M., Ruiz, S., & Astroza, R. (2012). Damage Assessment and Seismic Intensity Analysis of the 2010 (M-w 8.8) Maule Earthquake. *Earthquake Spectra, 28*. doi: 10.1193/1.4000027

Barnhart, W. D., Hayes, G. P., & Wald, D. J. (2019). Global Earthquake Response with Imaging Geodesy: Recent Examples from the USGS NEIC. *Remote Sensing, 11*(11), 1357.

Beck, S., Barrientos, S., Kausel, E., & Reyes, M. (1998). Source characteristics of historic earthquakes along the central Chile subduction Askew et Alzone. *Journal of South American Earth Sciences, 11*(2), 115-129.

Bradley, K., Mallick, R., Andikagumi, H., Hubbard, J., Meilianda, E., Switzer, A., . . . Benazir, B. (2019). Earthquake-triggered 2018 Palu Valley landslides enabled by wet rice cultivation. *Nature Geoscience*, 1-5.

Budimir, M. E. A., Atkinson, P. M., & Lewis, H. G. (2014). Earthquake-and-landslide events are associated with more fatalities than earthquakes alone. *Natural Hazards, 72*(2), 895-914. doi: 10.1007/s11069-014-1044-4

Carvajal, M., Araya-Cornejo, C., Sepúlveda, I., Melnick, D., & Haase, J. S. (2018). Nearly instantaneous tsunamis following the Mw 7.5 2018 palu earthquake. *Geophysical Research Letters, 46*(10): 5117-5126. doi: 10.1029/2019gl082578

Carver, G., Plafker, G., Metz, M., Cluff, L., Slemmons, B., Johnson, E., . . . Sorensen, S. (2004). Surface Rupture on the Denali Fault Interpreted from Tree Damage during the 1912 Delta River Mw 7.2–7.4 Earthquake: Implications for the 2002 Denali Fault Earthquake Slip Distribution. *Bulletin of the Seismological Society of America, 94*(6B), S58-S71. doi: 10.1785/0120040625

Cisternas, M., Atwater, B. F., Torrejón, F., Sawai, Y., Machuca, G., Lagos, M., . . . Kamataki, T. (2005). Predecessors of the giant 1960 Chile earthquake. *Nature, 437*(7057), 404.

Cisternas, M., Carvajal, M., Wesson, R., Ely, L. L., & Gorigoitia, N. (2017a). Exploring the Historical Earthquakes Preceding the Giant 1960 Chile Earthquake in a Time-Dependent Seismogenic Zone. *Bulletin of the Seismological Society of America, 107*(6), 2664-2675. doi: 10.1785/0120170103

Cisternas, M., Garrett, E., Wesson, R., Dura, T., & Ely, L. (2017b). Unusual geologic evidence of coeval seismic shaking and tsunamis shows variability in earthquake size and recurrence in the area of the giant 1960 Chile earthquake. *Marine Geology, 385*, 101-113.

Colombelli, S., Allen, R. M., & Zollo, A. (2013). Application of real-time GPS to earthquake early warning in subduction and strike-slip environments. *Journal of Geophysical Research: Solid Earth, 118*(7), 3448-3461. doi: 10.1002/jgrb.50242

Davis, S., & Karsulovic, J. (1961). *Deslizamientos en el valle del río San Pedro provincia de Valdivia, Chile.* Paper presented at the Anales de la Facultad de Ciencias Físicas y Matemáticas.

Dura, T., Horton, B.P., Cisternas, M., Ely, L., Hong, I., Nelson, A.R., Wesson, R.L., Pilarczyk, J.E., Parnell, A.C., Nikitina, D. (2017). Subduction zone slip variability during the last millennium, south-central Chile. *Quat. Sci. Rev. 175*, 112e137.

De Ramón, A. & Larraín, J. (1979). Una metrología colonial para Santiago de Chile: de la medida castellana al sistema métrico decimal. *Historia (Santiago: Instituto de Historia, Pontificia Universidad Católica de Chile), 14*, 5-71.

General Direction for Water. (2019). Official Hydrometeorological and Water Quality Information Online. http://snia.dga.cl/BNAConsultas/reportes

Gorum T., Fan X., van Westen, C.J., Huang, R.Q., Xu Q., Tang, C., & Wang, G. (2011). Distribution pattern of earthquake-induced landslides triggered by the 12 May 2008 Wenchuan earthquake. *Geomorphology, 133*(3-4):152–167. doi: 10.1016/j.geomorph.2010.12.030

Habit, E., & Parra, O. (2012). Fundamento y aproximación Metodológica del Estudio de peces del Río San Pedro. *Gayana (Concepción), 76*, 01-09.

Harp, E. L., Keefer, D. K., Sato, H. P., & Yagi, H. (2011). Landslide inventories: the essential part of seismic landslide hazard analyses. *Engineering Geology, 122*(1-2), 9-21.

Hauser, A. (2000). *Remociones en masa en Chile (versión actualizada)*: Servicio Nacional de Geología y Minería.

Hewitt, K. (1998). Catastrophic landslides and their effects on the Upper Indus streams, Karakoram Himalaya, northern Pakistan. *Geomorphology, 26*(1-3), 47-80.

548 Kanamori, H., & Cipar, J. (1974). Focal process of the great Chilean earthquake May 22, 1960.
549 *Physics of the Earth and Planetary Interiors, 9*(2), 128-136.

550 Keefer, D. (1984). Landslides caused by earthquakes. *GSA Bulletin, 95*(4), 406-421. doi:
551 10.1130/0016-7606(1984)95<406:LCBE>2.0.CO;2

552 Keefer, D. (2013). 5.11 Landslides Generated by Earthquakes: Immediate and Long-Term
553 Effects. In J. F. Shroder (Ed.), *Treatise on Geomorphology* (pp. 250-266). San Diego:
554 Academic Press.

555 Keefer, D., & Larsen, M. (2007). Assessing Landslide Hazards. *Science, 316*, 1136-1138. doi:
556 10.1126/science.1143308

557 Lay, T., Kanamori, H., Ammon, C. J., Koper, K. D., Hutko, A. R., Ye, L., . . . Rushing, T. M.
558 (2012). Depth-varying rupture properties of subduction zone megathrust faults. *Journal*
559 *of Geophysical Research: Solid Earth, 117*(B4). doi: 10.1029/2011jb009133

560 Lomnitz, C. (1970). Major earthquakes and tsunamis in Chile during the period 1535 to 1955.
561 *Geologische Rundschau, 59*(3), 938-960. doi: 10.1007/bf02042278

562 Mardones Flores, M., & Rojas Hernández, J. (2012). Procesos de remoción en masa inducidos
563 por el terremoto del 27F de 2010 en la franja costera de la Región del Biobío, Chile.
564 *Revista de Geografía Norte Grande*(53), 57-74.

565 Meteorological Direction of Chile. (2019). Climatological Yearbook.
566 https://climatologia.meteochile.gob.cl/application/index/anuarios

567 Moernaut, J., Daele, M. V., Heirman, K., Fontijn, K., Strasser, M., Pino, M., . . . De Batist, M.
568 (2014). Lacustrine turbidites as a tool for quantitative earthquake reconstruction: New
569 evidence for a variable rupture mode in south central Chile. *Journal of Geophysical*
570 *Research: Solid Earth, 119*(3), 1607-1633. doi: 10.1002/2013jb010738

571 Moernaut, J., Van Daele, M., Fontijn, K., Heirman, K., Kempf, P., Pino, M., Valdebenito, G.,
572 Urrutia, R., Strasser, M., De Batist, M. 2018. Larger earthquakes recur more periodically:
573 New insights in the megathrust earthquake cycle from lacustrine turbidite records in
574 south-central Chile. *Earth and Planetary Science Letters 481*, 9-19.

575 Montessus de Ballore, F. (1912). Historia sísmica de los Andes Meridionales al sur del paralelo
576 XVI. Segunda parte. Imprenta Cervantes. *Santiago*.

577 Moreno, M., Li, S., Melnick, D., Bedford, J., Baez, J., Motagh, M., . . . Gutknecht, B. (2018).
578 Chilean megathrust earthquake recurrence linked to frictional contrast at depth. *Nature*
579 *Geoscience, 11*(4), 285.

580 National Seismological Center of Chile. (2019). Great earthquakes in Chile.
581 https://www.csn.uchile.cl/sismologia/grandes-terremotos-en-chile/

582 Noguera, C., & Garcés, E. (1991). *Deslizamiento en el río San Pedro, analizado 30 años*
583 *después.* Paper presented at the Memorias, 9o Congreso Panamericano de Mecánica de
584 Suelos e Ingeniería de Fundaciones, Viña del Mar, Chile.

585 Ojala, A. E., Mattila, J., Markovaara-Koivisto, M., Ruskeeniemi, T., Palmu, J.-P., & Sutinen, R.
586 (2017). Distribution and morphology of landslides in northern Finland: An analysis of
587 postglacial seismic activity. *Geomorphology*. doi: 10.1016/j.geomorph.2017.08.045

588 Rodríguez, C., Pérez, Y., Moreno, H., Clayton, J., Antinao, J., Duhart, P., & Martin, M. (1999).
589 Area de Panguipulli-Riñihue, Región de Los Lagos. *Servicio Nacional de Geología y*
590 *Minería, Mapas Geológicos, 10*(1).

591 Ruiz, S., & Madariaga, R. (2018). Historical and recent large megathrust earthquakes in Chile.
592 *Tectonophysics, 733*, 37-56.

593 Scholz, C. H. (2002). *The Mechanics of Earthquakes and Faulting* (2 ed.). Cambridge:
594 Cambridge University Press.

595 Sepúlveda, S. A., Serey, A., Lara, M., Pavez, A., & Rebolledo, S. (2010). Landslides induced by
596 the April 2007 Aysén Fjord earthquake, Chilean Patagonia. *Landslides, 7*(4), 483-492.
597 doi: 10.1007/s10346-010-0203-2

598 Serey, A., Piñero-Feliciangeli, L., Sepúlveda, S. A., Poblete, F., Petley, D. N., & Murphy, W.
599 (2019). Landslides induced by the 2010 Chile megathrust earthquake: a comprehensive
600 inventory and correlations with geological and seismic factors. *Landslides, 16*(6), 1153-
601 1165. doi: 10.1007/s10346-019-01150-6

602 Silgado, E. (1985). Terremotos destructivos en America del Sur: 1530-1894. Centro Regional de
603 Sismología para America del Sur (CERESIS), 10, 328 p.

604 Symithe, S., & Calais, E. (2016). Present-day shortening in Southern Haiti from GPS
605 measurements and implications for seismic hazard. *Tectonophysics, 679*, 117-124.

606 U.S. Geological Survey (2016). M 7.6 - 41km SW of Puerto Quellon, Chile,
607 https://earthquake.usgs.gov/earthquakes/feed/v1.0/detail/us10007mn3.kml

608 Vanneste, K., Wils, K., & Van Daele, M. (2018). Probabilistic evaluation of fault sources based
609 on paleoseismic evidence from mass- transport deposits: the example of Aysén Fjord,
610 Chile. *Journal of Geophysical Research: Solid Earth*, *123*, 9842–9865. https://doi.org/
611 10.1029/2018JB016289

612 Watkinson, I. M., & Hall, R. (2019). Impact of communal irrigation on the 2018 Palu
613 earthquake-triggered landslides. *Nature Geoscience*, 1-6.

614 Weischet, W. (1963). Further observations of geologic and geomorphic changes resulting from
615 the catastrophic earthquake of May 1960, in Chile. *Bulletin of the Seismological Society*
616 *of America, 53*(6), 1237-1257.

617 Wright, C., & Mella, A. (1963). Modifications to the soil pattern of South-Central Chile resulting
618 from seismic and associated phenomenona during the period May to August 1960.
619 *Bulletin of the Seismological Society of America, 53*(6), 1367-1402.

620 Wu, W., & Sidle, R. C. (1995). A Distributed Slope Stability Model for Steep Forested Basins.
621 *Water Resources Research, 31*(8), 2097-2110. doi: 10.1029/95wr01136

622